Pavel Krejčí; Lenka Siváková; Jan Chleboun

Modelled behaviour of granular material during loading and unloading

In: Jan Chleboun and Pavel Kůs and Petr Přikryl and Miroslav Rozložník and Karel Segeth and Jakub Šístek and Tomáš Vejchodský (eds.): Programs and Algorithms of Numerical Mathematics, Proceedings of Seminar. Hejnice, June 24-29, 2018. Institute of Mathematics CAS, Prague, 2019. pp. 81–88.

Persistent URL: http://dml.cz/dmlcz/703079

Programs and Algorithms of Numerical Mathematics 19
J. Chleboun, P. Kůs, P. Přikryl, M. Rozložník, K. Segeth, J. Šístek, T. Vejchodský (Eds.)
Institute of Mathematics CAS, Prague 2019

MODELLED BEHAVIOUR OF GRANULAR MATERIAL DURING LOADING AND UNLOADING

Pavel Krejčí, Lenka Siváková, Jan Chleboun

Faculty of Civil Engineering, Czech Technical University
Thákurova 7, 166 29 Praha 6, Czech Republic
krejci@math.cas.cz, jan.chleboun@cvut.cz, lenka.sivakova@fbi.uniza.sk

Abstract: The main aim of this paper is to analyze numerically the model behaviour of a granular material during loading and unloading. The model was originally proposed by D. Kolymbas and afterward modified by E. Bauer. For our purposes the constitutive equation was transformed into a rate independent form by introducing a dimensionless time parameter. By this transformation we were able to derive explicit formulas for the strain-stress trajectories during loading-unloading cycles and compare the results with experiments. We were particularly interested in the observation of a special behaviour called ratchetlike motion in vibrated granular materials.

Keywords: granular materials, hypoplasticity, ratcheting

MSC: 74E20, 74C15, 74L10

1. Introduction

An introduction into the study of the asymptotic behaviour of stress trajectories under proportional loading and unloading can be found in [2]. The rate-independent transformation of the model describing hypoplasticity used in [7], [8] is enriched by the hypoplasticity hypothesis. This concept was already studied from the engineering point of view in [3], [5], [6], [9], [10], [11], [12] with a great attention to the phenomenon of *ratcheting*, see [1]. This phenomenon has the strongest agreement with reality for rate-independent constitutive models describing the behaviour of loading and unloading of granular materials. The mathematical techniques for proving the well-posedness of the model presented in the next section can be found in [4].

DOI: 10.21136/panm.2018.09

2. The Bauer model

Investigation of the inner processes in granular material during loading and unloading is based on the model from [2]. The strain-stress law is considered in the form

$$\dot{\boldsymbol{\sigma}} = c_1 \left(\dot{\boldsymbol{\varepsilon}} a^2 \operatorname{tr} \boldsymbol{\sigma} + \frac{\boldsymbol{\sigma}}{\operatorname{tr} \boldsymbol{\sigma}} (\boldsymbol{\sigma} : \dot{\boldsymbol{\varepsilon}}) + a(2\boldsymbol{\sigma} - \frac{1}{3}(\operatorname{tr} \boldsymbol{\sigma})\mathbf{I}) \|\dot{\boldsymbol{\varepsilon}}\| \right), \tag{1}$$

where $\boldsymbol{\varepsilon}$ is the strain tensor and $\boldsymbol{\sigma}$ is the stress tensor, both tensors are time-depentent, $\|\cdot\|$ stands for the Frobenius norm, $\mathbf{I}$ is the Kronecker tensor, $\operatorname{tr} \boldsymbol{\sigma} = \boldsymbol{\sigma} : \mathbf{I}$ is the trace of $\boldsymbol{\sigma}$, $a > 0$ is a model parameter, and $c_1 < 0$ is a scaling parameter which, as we shall see, has no influence on the asymptotic behaviour of the model. The dot represents the derivative with respect to time t. We consider proportional strain paths of the form

$$\boldsymbol{\varepsilon}(t) = \varepsilon(t)\mathbf{U}, \ \dot{\boldsymbol{\varepsilon}}(t) = \dot{\varepsilon}(t)\mathbf{U}, \tag{2}$$

where $\varepsilon(t) \colon [0, \infty) \to \mathbb{R}$ is a given function, and $\mathbf{U}$ is a fixed symmetric tensor

$$\mathbf{U} = \begin{pmatrix} u_{11} & u_{12} & u_{13} \\ u_{21} & u_{22} & u_{23} \\ u_{31} & u_{32} & u_{33} \end{pmatrix}. \tag{3}$$

This is what we call a *proportional loading*. The tensor $\mathbf{U}$ can be physically interpreted as the direction of stress paths during loading and unloading.

Hypothesis 1. *Our analysis of equation (1) will be carried out under the following hypotheses:*

(i) *the material is initially compressed, that is, $\boldsymbol{\sigma}(0)$ is a given tensor such that $\langle \boldsymbol{\sigma}(0), \mathbf{I} \rangle < 0$, where $\langle \cdot, \cdot \rangle$ is the Frobenius inner product;*

(ii) *we investigate below the different dynamics of the model under increasing compression (or loading) corresponding to $\langle \mathbf{U}, \mathbf{I} \rangle > 0$, decreasing compression (or unloading) corresponding to $\langle \mathbf{U}, \mathbf{I} \rangle < 0$, and volume preserving compression corresponding to $\langle \mathbf{U}, \mathbf{I} \rangle = 0$;*

(iii) *$\varepsilon \colon [0, \infty) \to \mathbb{R}$ is absolutely continuous, $\dot{\varepsilon}(t) < 0$ for a. e. $t > 0$, $\lim_{t \to \infty} \varepsilon(t) = -\infty$.*

By introducing a time transformation $s(t)$ by the formula

$$\dot{s}(t) = c_1 \dot{\varepsilon}(t), \quad s(0) = 0, \text{ and } \boldsymbol{\sigma}'(s) = \frac{\mathrm{d}\boldsymbol{\sigma}}{\mathrm{d}s},$$

we transform equation (1) into a rate-independent form:

$$\begin{aligned} \boldsymbol{\sigma}' &= a^2 \langle \boldsymbol{\sigma}, \mathbf{I} \rangle \mathbf{U} + \frac{\langle \boldsymbol{\sigma}, \mathbf{U} \rangle}{\langle \boldsymbol{\sigma}, \mathbf{I} \rangle} \boldsymbol{\sigma} - a \|\mathbf{U}\| \left(2\boldsymbol{\sigma} - \frac{1}{3} \langle \boldsymbol{\sigma}, \mathbf{I} \rangle \mathbf{I} \right) \\ &= \langle \boldsymbol{\sigma}, \mathbf{I} \rangle \left(a^2 \mathbf{U} + \frac{a}{3} \|\mathbf{U}\| \mathbf{I} \right) + \boldsymbol{\sigma} \left(\frac{\langle \boldsymbol{\sigma}, \mathbf{U} \rangle}{\langle \boldsymbol{\sigma}, \mathbf{I} \rangle} - 2a \|\mathbf{U}\| \right). \end{aligned} \tag{4}$$

3. Model analysis

The solution of (4) for each fixed constant tensor $\mathbf{U}$ (see [2]) admits an explicit representation in the form:

$$\boldsymbol{\sigma}(s) = \mathrm{e}^{g(s)}\boldsymbol{\sigma}(0) + \frac{\langle \boldsymbol{\sigma}(0), \mathbf{I}\rangle}{\langle \mathbf{V}, \mathbf{I}\rangle}\left(\mathrm{e}^{f(s)} - \mathrm{e}^{g(s)}\right)\mathbf{V}\,, \tag{5}$$

with functions

$$f(s) = Ds + \frac{C}{\eta}(1 - \mathrm{e}^{-\eta s}), \quad g(s) = (B - 2a\|\mathbf{U}\|)s + \frac{C}{\eta}(1 - \mathrm{e}^{-\eta s}), \tag{6}$$

where

$$\mathbf{V} = a^2\mathbf{U} + \frac{a}{3}\|\mathbf{U}\|\mathbf{I}, \tag{7}$$

$$B = \frac{\langle \mathbf{V}, \mathbf{U}\rangle}{\langle \mathbf{V}, \mathbf{I}\rangle}, \tag{8}$$

$$C = \frac{\langle \boldsymbol{\sigma}(0), \mathbf{U}\rangle}{\langle \boldsymbol{\sigma}(0), \mathbf{I}\rangle} - B, \tag{9}$$

$$\eta = a\|\mathbf{U}\| + a^2\langle \mathbf{V}, \mathbf{U}\rangle\,, \tag{10}$$

$$D = \frac{a^3\langle \mathbf{U}, \mathbf{I}\rangle^2 + \frac{1}{3}\|\mathbf{U}\|\langle \mathbf{U}, \mathbf{I}\rangle}{\|\mathbf{U}\| a\langle \mathbf{U}, \mathbf{I}\rangle}. \tag{11}$$

According to formula (5), the tensor $\mathbf{V}$ represents the asymptotic stress direction as long as $g(s) < 0$. A discussion in [2] shows that only the parameter values

$$a > \frac{1}{2\sqrt{3}} \approx 0.289 \tag{12}$$

lead to a good qualitative agreement with experiments, and are therefore physically relevant.

In the numerical examples in Section 4, we consider loading/unloading processes in two opposite directions $\mathbf{U}$ that we denote $\mathbf{U}^+$ for loading, and $\mathbf{U}^- = -\mathbf{U}^+$ for unloading. We let the dimensionless time s vary within fixed bounded intervals $[0, S^+]$, $[0, S^-]$, respectively. The corresponding asymptotic directions $\mathbf{V}$ in (7) are denoted accordingly $\mathbf{V}^+, \mathbf{V}^-$.

4. Numerical examples

From the observation of the behaviour of the model for different parameter values, we were able to categorize these types: cyclic case, convergence to zero, divergence to infinity, isotropic case, and fast divergence to infinity when the physical condition (12) is violated. For each type of behaviour we choose typical values of parameters for which the behaviour can be observed and graphed. We consider only diagonal tensors $\mathbf{U}, \boldsymbol{\sigma}$ and represent them in the tables by 3D vectors.

Cyclic case

Ratcheting is observed in cyclic processes when the mechanical response to a time-periodic input exhibits shifts in the phase space. In the case of Figure 1, the stress path asymptotically converges to the plane determined by the two asymptotic directions $\mathbf{V}^+, \mathbf{V}^-$ and represented by the grey parallelogram. The values of the variables can be found in Table 1.

variables	S^+	S^-	$\mathbf{U}^+$	$\boldsymbol{\sigma}(0)$	a
values	1	0.2	$(1,0,0)$	$(10,10,10)$	0.5

Table 1: Cyclic case.

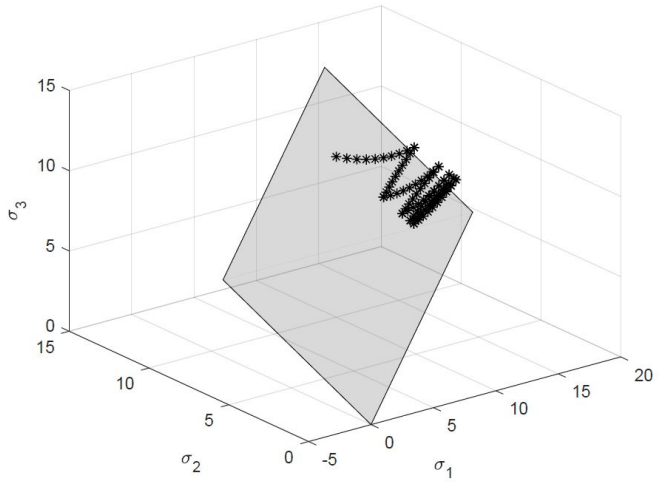

Figure 1: Cyclic case.

Convergence to zero

The case when the stress path converges to zero corresponds to a stable state of inner processes during loading and unloading. It means that the resting phase, or, in other words, the stress relaxation during unloading is dominant. In this case the stress paths converge asymptotically to zero, see Figure 2. The values of the variables can be found in Table 2.

Divergence to infinity

In the case when the stress relaxation during the unloading phase is dominated by the stress increase during loading, the stress path diverges to infinity, see Figure 3. The values of the variables can be found in Table 3.

variables	S^+	S^-	$\mathbf{U}^+$	$\boldsymbol{\sigma}(0)$	a
values	1	0.5	$(1,0,0)$	$(10,10,10)$	0.5

Table 2: Convergence to zero.

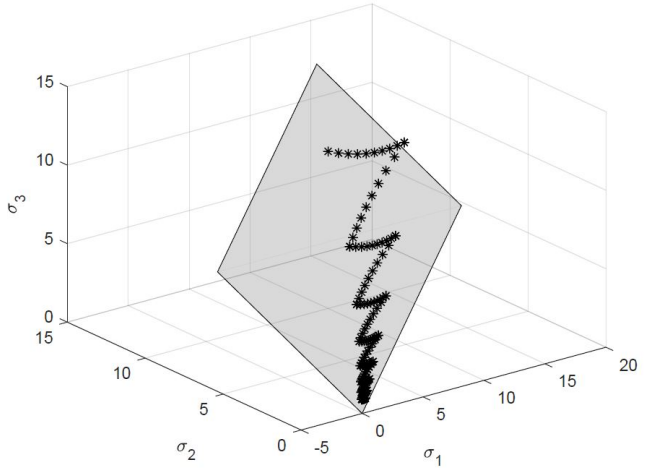

Figure 2: Convergence to zero.

variables	S^+	S^-	$\mathbf{U}^+$	$\boldsymbol{\sigma}(0)$	a
values	1	0.1	$(1,0,0)$	$(10,10,10)$	0.5

Table 3: Divergence to infinity.

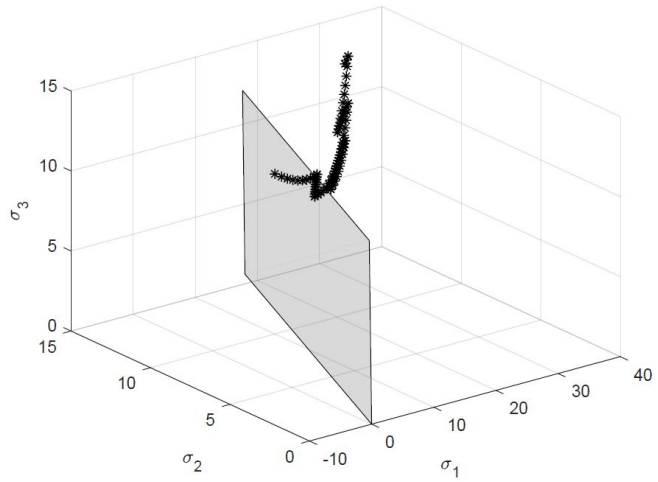

Figure 3: Divergence to infinity.

Violation of the physical condition

This example demonstrates what can happen if the condition $a > 1/2\sqrt{3}$ from (12) is violated. We see in Figure 4 that the stress paths quickly diverge to infinity and the process is very unstable. The values of the variables can be found in Table 4.

variables	S^+	S^-	$\mathbf{U}^+$	$\boldsymbol{\sigma}(0)$	a
values	1	0.2	$(1,0,0)$	$(10,10,10)$	0.1

Table 4: Violation of the condition $a > 1/2\sqrt{3}$.

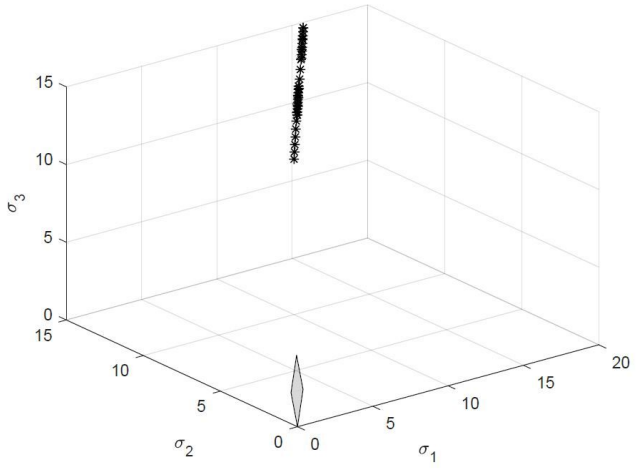

Figure 4: Violation of the condition $a > 1/2\sqrt{3}$.

Isotropic case

This is an example of strain ratcheting. The values of S^+ and S^- are computed in terms of the ratio between D and $B - 2a$ for given a and $\boldsymbol{\sigma}(0)$ so as to get a periodic stress path up and down along the isotropic direction $\mathbf{I}$ as in Figure 5. The ratio S^+/S^- characterizes the strain ratcheting rate along $\mathbf{I}$. The values of the variables can be found in Table 5.

variables	S^+	S^-	$\mathbf{U}^+$	$\boldsymbol{\sigma}(0)$	a
values	1	0.338	$(1,1,1)$	$(10,10,10)$	0.5

Table 5: Isotropic case.

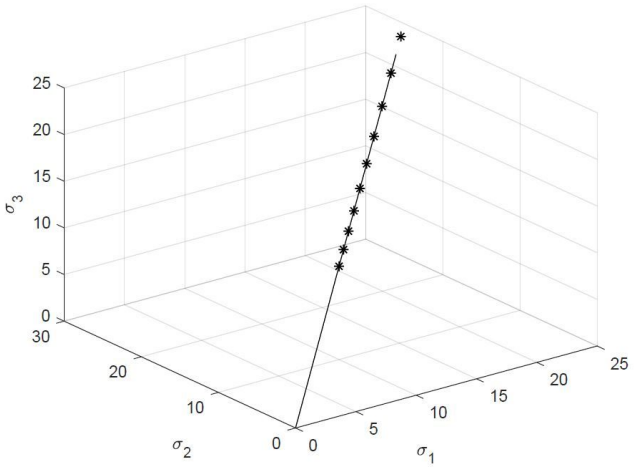

Figure 5: Isotropic case.

5. Conclusion

By using numerical methods we model different types of behaviour of granular material during loading and unloading. These types of behaviour can be categorized as: cyclic case, convergence to zero, divergence to infinity, isotropic case, and fast divergence to infinity when physical conditions are violated. Strain ratcheting with a good qualitative and quantitative agreement with experiments is observed in the isotropic case.

Acknowledgements

This work was supported by the Project No. 7AMB16AT035 within the MSMT Mobility Programme (Austria), by the Grant Agency of the Czech Technical University in Prague, grant No. SGS18/006/OHK1/1T/11, and by the European Regional Development Fund under Project No. CZ.02.1.01/0.0/0.0/16_019/0000778.

References

[1] Alonso-Marroquín, F. and Herrmann, H. J.: Ratcheting of granular materials. Phys. Rev. Lett. **92** (2004), 054301.

[2] Bauer, E., Kovtunenko, V.A., Krejčí, P., Siváková, L., and Zubkova, A.: On Lyapunov stability in hypoplasticity. In: K. Mikula, D. Ševčovič, and J. Urbán (Eds.), *Proceedings of Equadiff 2017 Conference*, pp. 107–116. Slovak University of Technology, SPEKTRUM STU Publishing, Bratislava, 2017.

[3] Bauer, E. and Wu, W.: A hypoplastic model for granular soils under cyclic loading. In: D. Kolymbas (Ed.), *Modern approaches to plasticity*, pp. 247–258. Elsevier, Amsterdam, 1993.

[4] Brokate, M. and Krejčí, P.: Wellposedness of kinematic hardening models in elastoplasticity. ESAIM Math. Model. Numer. Anal. **32** (1998), 177–209.

[5] Gudehus, G.: *Physical soil mechanics*. Springer-Verlag, Berlin, 2011.

[6] Huang, W. and Bauer, E.: Numerical investigations of shear localization in a micro-polar hypoplastic material. Int. J. Numer. Anal. Met. **27** (2003), 325–352.

[7] Kolymbas, D.: *Introduction to hypoplasticity*. Taylor & Francis, London, 2000.

[8] Kolymbas, D.: *Constitutive modelling of granular materials*. Springer-Verlag, Berlin, 2000.

[9] Krejčí, P., O'Kane, P., Pokrovskii, A., and Rachinskii, D.: Stability results for a soil model with singular hysteretic hydrology. J. Phys.: Conf. Ser. **268** (2011), 012016.

[10] Niemunis, A. and Herle, I.: Hypoplastic model for cohesionless soils with elastic strain range. Mech. Cohes.-Frict. Mat. **2** (1997), 279–299.

[11] Svendsen, B., Hutter, K., and Laloui, L.: Constitutive models for granular materials including quasi-static frictional behaviour: Toward a thermodynamic theory of plasticity. Contin. Mech. Thermodyn. **11** (1999), 263–275.

[12] Wu, W., Bauer, E., and Kolymbas, D.: Hypoplastic constitutive model with critical state for granular materials. Mech. Mater. **23** (1996), 45–69.